analytical chemistry

Article

pubs.acs.org/ac

DNA–Gold Nanoparticle Conjugates-Based Nanoplasmonic Probe for Specific Differentiation of Cell Types

Xiafeng Yang,[†,§,‡] Jiang Li,[§,‡] Hao Pei,[§] Yun Zhao,[†] Xiaolei Zuo,[§] Chunhai Fan,[§] and Qing Huang*[,§]

[†]College of Life Science, Sichuan University, Chengdu, Sichuan 610064, China

[§]Division of Physical Biology & Bioimaging Center, Shanghai Synchrotron Radiation Facility, Shanghai Institute of Applied Physics, Chinese Academy of Sciences, Shanghai, 201800, China

ABSTRACT: The direct analysis of cancerous cells provides a new way for cancer detection that obviates cell lysis and other tedious steps (e.g., enrichment, purification, and amplification steps). However, the analysis of different cell types remains challenging due to the subtle differences in cell surface features. Here, we have demonstrated nanoplasmonic differentiation of cell types by using DNA–gold nanoparticle nanoconjugates (DNA-AuNPs). Our strategy relies on cross reactive receptors (a collection of DNA-AuNPs) that are employed to bind the different cells that produce fingerprint-like patterns for each type of cell. Because of the enhanced nanoplasmonic effect of AuNPs via seeded-growth, we could effectively differentiate various cell lines, e.g., 786-O, L929, Hela, and RAW264.7, with dark-field microscopy or even naked eyes.

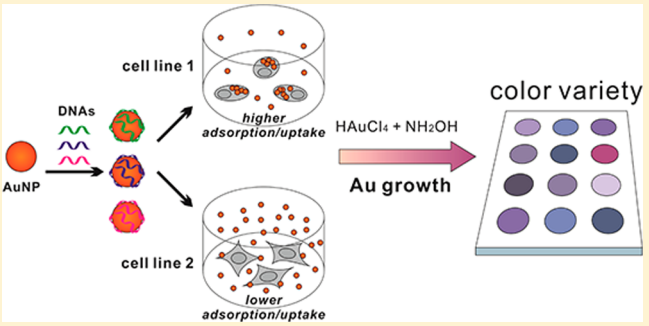

Early detection of cancer is crucially important for diagnosis, prognosis, and therapy.[1,2] Sensitive detection of molecular biomarkers is a representative approach for the cancer detection.[1−4] It usually requires the lysis of cancer cells and the subsequent enrichment, purification, and amplification steps (e.g., for the detection of DNA, microRNA, and telomerase). The direct analysis of cancerous cells provides a new way for cancer detection that obviates the cell lysis and other tedious steps.[5−8] However, the analysis of different cell types remains challenging due to the subtle differences in cell surface features. For example, the analysis and isolation of circulating tumor cells (CTCs) are simply based on the size of CTCs or the epithelial cell adhesion molecule (EpCAM, a nearly universal biomarker for tumor cells), which raises the problem of low specificity and accuracy for cell type analysis.[9] Therefore, it is urgent to develop an efficient platform for cell type analysis, which is characterized with simple design and inexpensive readout.

The traditional method for cell type analysis usually requires molecular ligands (e.g., antibodies and aptamers) that are highly specific to target cells.[10,11] The production of the specific ligands (e.g., in vitro systematic evolution of ligands by exponential enrichment, SELEX) and the design of specific sensors are usually expensive and time-consuming. To circumvent this, cross reactive receptors have been employed to bind the analytes that produce fingerprint-like patterns for each analyte.[6,12−19] This is what nature does to develop olfactory neural systems such as smell that use differential binding. This strategy does not require the development of high specific receptors to the analyte. Some examples have demonstrated that assembling a group of weakly selective receptors into an integrated recognizing system with high specificity makes analysis independent of specific ligands.

However, the preparation, design, and synthesis of receptors are still limitations for the ligands independent system.[15] Here, we creatively proposed a strategy that modulates the preparation of receptors, through which the receptors can be easily prepared by mixing some basic blocks. We assembled gold nanoparticles (AuNPs) and DNA sequences (with different composition and length) to DNA–gold nanoparticle conjugates (DNA-AuNPs) as the basic blocks. A collection of receptors can be prepared through the combination of these blocks. Our modulation strategy will significantly simplify the process of preparing receptors.

Interactions between DNA-AuNPs and living cells (adsorption and internalization) play fundamentally critical roles in some practical applications like cellular diagnosis and drug delivery, which have attracted extensive research interest in recent years.[20−22] It has been proved that DNA-AuNPs can be internalized by mammalian cells, while the efficiency of which varies among different types of cells, and is related to the density of DNAs on the surface of nanoparticles. On the basis of which, we propose a novel strategy for cell analysis based on DNA-AuNPs nanoconjugates, which is easy for preparation and use. After incubation of nanoconjugates with cells, the quantity of nanoconjugates adsorbed and internalized by different cells varies, and this variation can be further amplified by seed mediated growth of AuNPs via the reduction of $HAuCl_4$. The resulting colors as fingerprint-like patterns are employed to discriminate different cell types, which provide a simple, optical,

Received: February 3, 2014
Accepted: February 24, 2014
Published: February 24, 2014

   dx.doi.org/10.1021/ac500381e | *Anal. Chem.* 2014, 86, 3227−3231

Scheme 1. Schematic Illustration of Nanoplasmonic Differentiation of Cell Types by Using DNA-AuNPs

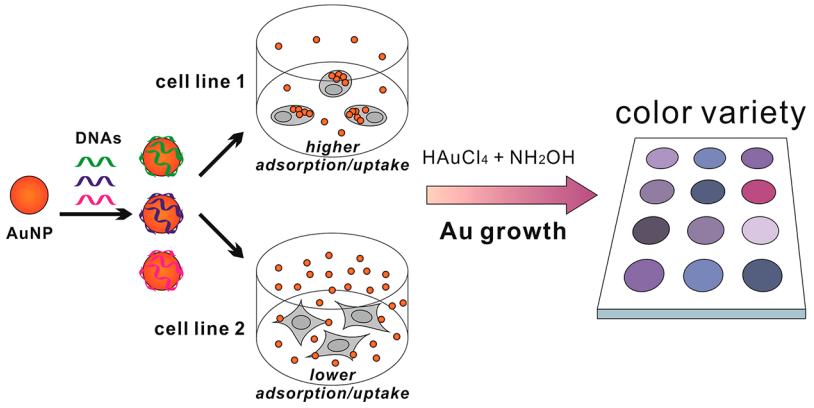

and inexpensive way for the differentiation of cell types (Scheme 1).

RESULTS AND DISCUSSION

Colorimetric Assay of Seed-Mediated Growth of AuNPs for Quantitative Analysis of AuNPs. The characteristic color of AuNPs originated from surface plasmon resonance (SPR) has long been an excellent tool for tremendous biomedical applications.[23−28] For example, many optical biosensing strategies employ the color-shift of AuNPs as their readouts, which is sensitively responsive to the change of interspace among particles, shape, or particle sizes. However, when the molar concentration of AuNPs is very low, the color of AuNPs is too light to be discriminated. Hence, in this situation, mass spectrometry-related methods are often employed for quantification of Au atoms, as described by many previous studies about cellular uptake of Au-based materials. These methods are relatively cumbersome and need complicated instruments.

AuNPs themselves can serve as seeds[29] in the reaction of $HAuCl_4$ and a reductant (in this study, NH_2OH), which catalyzes the growth of gold on seeding AuNPs. Moreover, the seed-mediated growth of AuNPs can dramatically enhance the surface plasmon resonance and, thus, strengthen the color of AuNPs. Even when AuNPs are densely coated with other biomolecules like DNAs and proteins, this seed-mediated growth reaction is still able to proceed.

Here, we prepared polyA-AuNPs by simply incubating polyAs (oligonucleotides containing consecutive adenines) of different lengths and citrate-stabilized AuNPs (13 nm in diameter, 20 nM in concentration). Then, these polyA-AuNPs were employed as seeds and allowed to catalyze the growth of gold. Before growth, the solutions of polyA-AuNPs (picomolar) were almost as clear as water (Figure 1). However, after growth, the colors of solutions were strengthened dramatically to discernible depths (Figure 1). More importantly, the absorbance of resulting solutions (we employed the absorbance at 600 nm for measuring) presented by grown nanoparticles was positively related to the initial molar concentration of AuNPs within a wide range (from 0.06 to 200 pM, over 3 orders of magnitude). Therefore, the seed-mediated growth of AuNPs could be employed as a convenient amplification method for quantification of AuNPs at low concentration.

Interactions between Cells and AuNPs Coated with polyAs. We previously demonstrated that the density of DNA on the surface of AuNPs could be regulated by tuning the length of polyA.[30] Here, polyAs of various lengths (10A, 20A, 30A, 60A) were employed for preparing different polyA-AuNPs, by simply mixing overdosed polyA oligonucleotides with citrate-stabilized AuNPs (13 nm in diameter). Meanwhile, as a control, PEG-coated AuNPs (PEG-AuNPs) were prepared. Thereafter, we incubated living cells (MCF-7, human breast cancer cell) with these different polyA-AuNPs for 4 h and then monitored the cells with dark-field microscopy. As verification, we also quantified the amount of Au retained by cells via inductively coupled plasma-atomic emission spectrometry (ICP-AES). We observed that the cells treated with polyA-AuNPs presented obviously more red-colored spots as compared to those treated with PEG-AuNPs, indicating more interactions of PolyA-AuNPs and the cells. Quantification analysis by ICP-AES (Figure 2) confirmed that the polyA-AuNPs retained by cells increased along with the increase of the length of polyA.

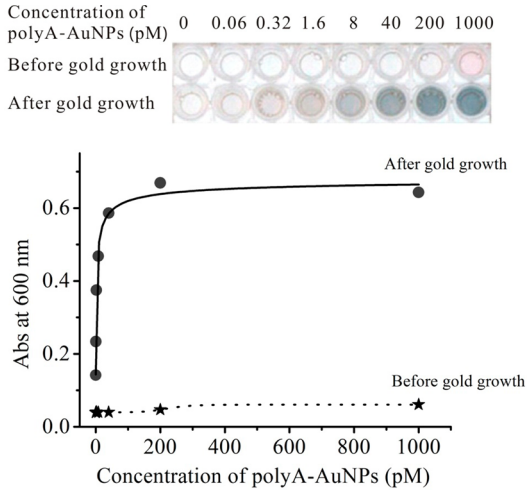

Figure 1. (top) The color of gold nanoparticles at picomolar concentrations is light due to the low concentration. After the catalytic seeded gold growth, the surface plasmon resonance is enhanced. The final color presented by the grown AuNPs is correlated to the initial concentration of AuNPs. (bottom) The relation between absorbance values of polyA-AuNPs after growth and their initial molar concentrations.

Visible Variation from Au Growth Reaction between Different Cell Lines. For comparison, another cell line RAW264.7 (As a macrophage cell line, it is known for its nature of devouring invasive materials like infectious microbes and cancer cells.) was employed to interact with PolyA-AuNPs.

dx.doi.org/10.1021/ac500381e | Anal. Chem. 2014, 86, 3227−3231

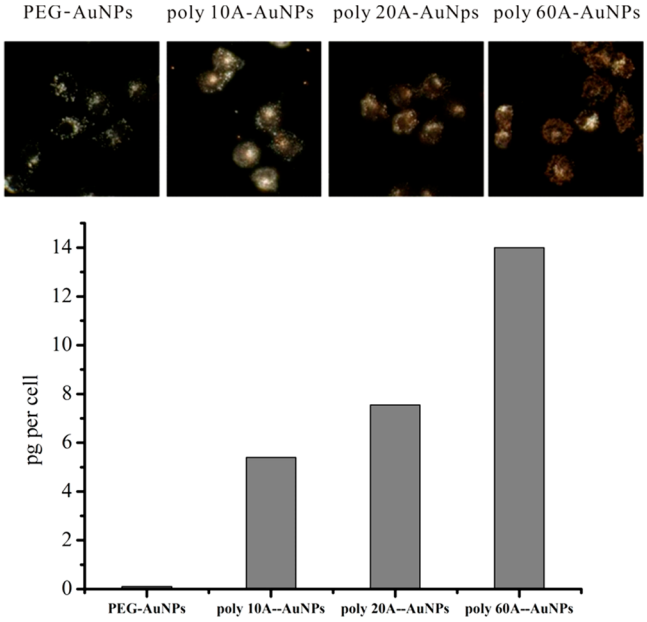

Figure 2. (top) Images of dark-field microscopy demonstrated that MCF-7 cells interact differently with PEG-AuNPs, poly 10A-AuNPs, poly 20A-AuNPs, and poly 60A-AuNPs. Along with the increasing DNA length, the AuNPs that were retained on the cell surface increase. (bottom) The amount of Au on the cell (detected through ICP-AES) verified that the poly 60A-AuNPs have strong interaction with MCF-7 cells. The PEG-AuNPs have weak interaction with MCF-7 cells.

After the treatment with polyA-AuNPs (AuNPs were coated with 10A or 60A), we observed that the cells of RAW264.7 demonstrated a much higher retention of both kinds of polyA-AuNPs as compared to the cells of MCF-7 (Figure 3). The quantification by ICP-AES (Figure 3) verified this phenomenon. This should contribute to the extraordinary high activity of internalization presented by RAW264.7 cells. With a colorimetric assay of AuNPs after the growth reaction (Figure 3), the light absorbance of grown particles resulted from the RAW264.7 cells was significantly higher than that from MCF-7, indicating the AuNPs retained by RAW264.7 were much more than those retained by MCF-7. These colorimetric results were not only in accordance with those from dark-field microscopy and ICP-AES but also discernible with the naked eyes.

Identification of Different Cells with Visualized Fingerprints. On the basis of the successful cell type differentiation of MCF-7 and RAW264.7, we can employ our strategy to differentiate many other cell types. To realize this, we prepared a series of basic blocks through the assembly of Au-NPs and Poly A, Poly C (oligonucleotides containing consecutive cytosines), and Poly T (oligonucleotides containing consecutive thymines). With these basic blocks, a collection of receptors can be easily prepared by combining some of these basic blocks. As the test bed, we employed polyA10-AuNPs, polyA30-AuNPs, polyT10-AuNPs, polyT30-AuNPs, polyC30-AuNPs, and bare AuNPs as a combination to differentiate four different cell types including 786-O (human kidney carcinoma cell line), L929 (murine aneuploid fibrosarcoma cell line), Hela (cervical cancer cell line), and RAW264.7. These cells seeded in 96-well plates were respectively treated with as-prepared six kinds of AuNPs. Then, without discarding the suspension (including culture medium and suspended AuNPs that had not

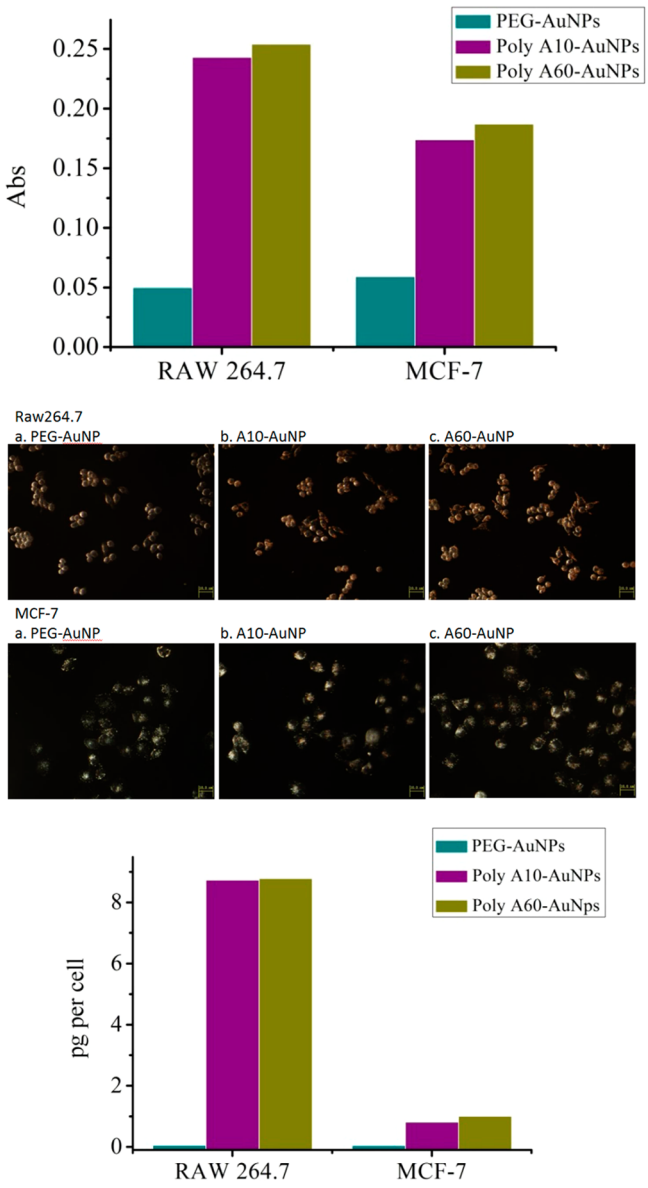

Figure 3. (top) The fingerprint-like patterns of absorbance values for RAW264.7 cell line and MCF-7 cell line. We can completely differentiate these two cell lines through the patterns. (middle) The corresponding images of dark-field microscopy demonstrated different colors of cells treated with different conjugates of AuNPs. (bottom) Our results were verified by ICP-AES that demonstrated different patterns for RAW264.7 cell line and MCF-7 cell line.

interacted with cells), $HAuCl_4$ and NH_2OH were directly added into the solution for seed-mediated gold growth. The absorbance after gold growth demonstrated a fingerprint-like pattern for each cell type (Figure 4). We obtained complete differentiation of the four cell types from these fingerprint patterns. Among these patterns, it is obvious that the overall absorbance values resulted from RAW264.7 cells were obviously lower than that from other nonphagocyte cell lines. We hypothesized that, in this test, the AuNPs suspended in the medium made a major contribution to the color enhancement, and because RAW264.7 cells could internalize much more AuNPs, the remaining AuNPs suspended in their medium should be less than others, causing the lighter colors after gold growth. The fingerprint pattern of each cell line was an 18

dx.doi.org/10.1021/ac500381e | Anal. Chem. 2014, 86, 3227−3231

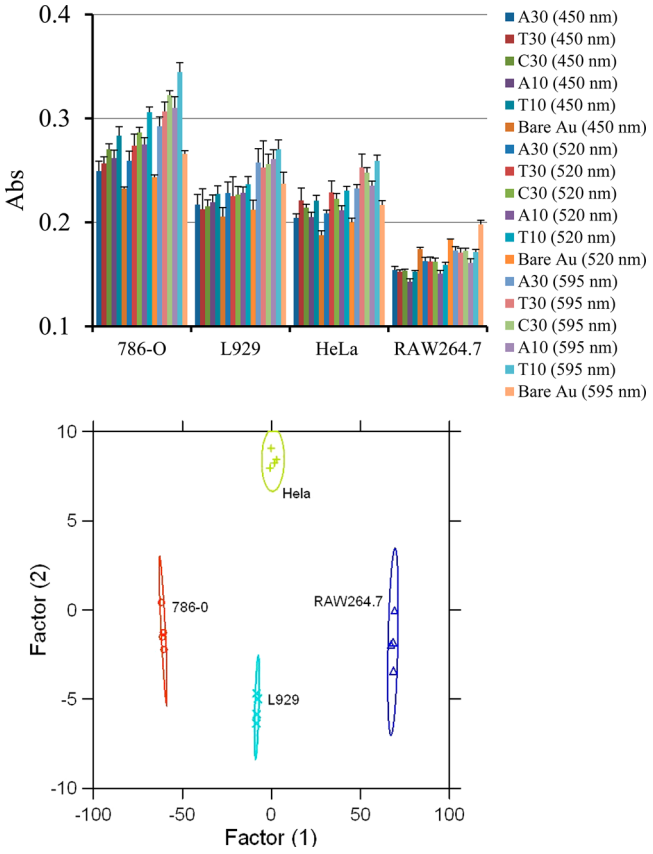

Figure 4. (top) A collection of DNA-AuNPs was employed to produce fingerprint-like patterns for four cell lines (768-O, L929, Hela, and Raw264.7). We obtained complete differentiation for these four different cell lines. (bottom) Canonical score plot for the four different cell lines (768-O, L929, Hela, and Raw264.7). The results demonstrated well-separated patterns.

dimensional (6 AuNPs × 3 wavelengths) data set containing characteristic information about the cell. We then employed linear discriminant analysis (LDA) to reduce the dimensionality of the data. The first two most significant discrimination factors resulted from LDA were used to generate a 2-D canonical score plot (Figure 4). As we can see, each cell line had four scattered points representing four independent samples and was surrounded by a 95% confidence ellipse. These ellipses representing different cell lines could be well isolated from each other. The results indicated that this method effectively identified different cell types from each other.

EXPERIMENTAL SECTION

Preparation of DNA-AuNPs. Oligonucleotides (sythesized by Life Technologies Co.) of different sequences (A10, A 20, A30, A60, T10, T30, and C30) were respectively quantified with a UV-spectrometer (HITACHI U-3010) and diluted to 100 μM with Milli-Q water. Citrate-stabilized AuNPs (13 nm) were prepared as described in previous literature. In brief, trisodium citrate solution (10 mg/mL, 3.5 mL) was added to a boiling, rapidly stirred solution of $HAuCl_4$ (1% w/v, 100 mL). The solution was kept boiling and stirred for 30 min. After being naturally cooled to room temperature, the AuNPs were filtered (with 0.22 μm Millipore membrane filter) and concentrated to 10 nM by centrifuging (15,000g, 30 min). For preparation of DNA-AuNPs, the oligonucleotide of a certain sequence was directly mixed with as-prepared AuNPs. The final molar concentration of polyA was 200-fold higher than AuNPs. The mixture was incubated on a shaking incubator (400 rpm, 25 °C) for 1 h, which was then used for cell treatment without further purification. For comparison, PEG-AuNPs were prepared using the same method, only replacing DNAs with SH-PEG (MW = 5000).

Cell Treatment and Characteristics. All cells in this study were obtained from Cell Bank of Shanghai Institute of Cell Biology, Chinese Academy of Sciences, and cultured following respective instructions supplied by the supplier. Before treatment, cells were seeded at certain density in a 96-well plate (6,000 cells per well) or 35 mm cell culture dishes (200,000 cells per dish), allowed to grow for 12 h, and then rinsed with PBS twice to remove their original culture medium. Next, these cells were treated with phenol red-free DMEM culture medium (Life Technologies Co.) containing polyA-AuNPs of a certain concentration, for 4 h at 37 °C. For AuNPs growth reaction and colorimetric assay, the treating medium was kept for further analysis; for dark field microscopy and ICP-AES, the medium was removed and the cells were rinsed with PBS at least four times. Dark field light-scattering images were acquired using an OLYMPUS IX71 inverted microscope coupled with an OLYMPUS DP70 digital camera. For ICP-AES quantification of Au, cells were further lysed with nitric acid. The dilution of which was analyzed by an inductively coupled plasma-atomic emission spectrometer (PerkinElmer). The content of AuNPs retained by cells was calculated on the basis of a calibration curve obtained from a group of AuNPs solution of known concentrations.

AuNPs Growth Reaction and Colorimetric Assay. After cell treatment, NH_2OH (0.1 M, 50 μL) and $HAuCl_4$ (0.1 mM, 50 μL) were successively added into the treating medium to induce the growth of AuNPs. Five minutes later, absorbance values of the mixture at 450, 520, and 600 nm were read by a BioTekSynergy H1 microplate reader. The colorimetric patterns resulted from the growth of AuNPs were analyzed by linear discriminant analysis (LDA) applying Mahalonobis clustering analysis, using the software Systat 12. LDA is a statistical method that transforms the raw response patters to canonical patters and maximizes the ratio of between-class variance to the within-class variance according to the preassigned grouping. After the analysis, four canonical factors were generated that represent linear combinations of the response matrices obtained from the absorbance response patterns (6 DNA-AuNPs × 4 cells × 4 replicates). The first two most significant discrimination factors were employed to generate a two-dimension plot.

CONCLUSION

In summary, we have developed a simple platform for nanoplamonic differentiation of cell types through DNA–gold nanoparticles conjugates. Our strategy possesses several advantages. First, the readout of our strategy is simply based on the color of AuNPs. Naked eye or simple UV-spectrometer is sufficient to differentiate different cell types. Second, the cross reactive receptors can be prepared by mixing some basic blocks, which are modulated DNA-AuNPs. Third, the "proof-of-principle" study could be generalized to many other cancerous cell types.

AUTHOR INFORMATION

Corresponding Author

*E-mail: huangqing@sinap.ac.cn. Fax: 021-39194173.

Author Contributions

‡Xiafeng Yang and Jiang Li contributed equally.

Notes

The authors declare no competing financial interest.

■ ACKNOWLEDGMENTS

This work was supported by National Natural Science Foundation of China (Grant No. 21105111) and Shanghai Municipal Natural Science Foundation (Grant No. 11ZR1445300).

■ REFERENCES

(1) Schwarzenbach, H.; Hoon, D. S. B.; Pantel, K. *Nat. Rev. Cancer* **2011**, *11*, 426−437.
(2) Boeri, M.; Verri, C.; Conte, D.; Roz, L.; Modena, P.; Facchinetti, F.; Calabro, E.; Croce, C. M.; Pastorino, U.; Sozzi, G. *Proc. Natl. Acad. Sci. U.S.A.* **2011**, *108*, 3713−3718.
(3) Li, D.; Song, S. P.; Fan, C. H. *Acc. Chem. Res.* **2010**, *43*, 631−641.
(4) Lubin, A. A.; Plaxco, K. W. *Acc. Chem. Res.* **2010**, *43*, 496−505.
(5) Bajaj, A.; Rana, S.; Miranda, O. R.; Yawe, J. C.; Jerry, D. J.; Bunz, U. H. F.; Rotello, V. M. *Chem. Sci.* **2010**, *1*, 134−138.
(6) Miranda, O. R.; Creran, B.; Rotello, V. M. *Curr. Opin. Chem. Biol.* **2010**, *14*, 728−736.
(7) Al-Hajj, M.; Wicha, M. S.; Benito-Hernandez, A.; Morrison, S. J.; Clarke, M. F. *Proc. Natl. Acad. Sci. U.S.A.* **2003**, *100*, 3983−3988.
(8) Miranda, O. R.; Li, X. N.; Garcia-Gonzalez, L.; Zhu, Z. J.; Yan, B.; Bunz, U. H. F.; Rotello, V. M. *J. Am. Chem. Soc.* **2011**, *133*, 9650−9653.
(9) Chen, W. Q.; Weng, S. N.; Zhang, F.; Allen, S.; Li, X.; Bao, L. W.; Lam, R. H. W.; Macoska, J. A.; Merajver, S. D.; Fu, J. P. *ACS Nano* **2013**, *7*, 566−575.
(10) Fang, X. H.; Tan, W. H. *Acc. Chem. Res.* **2010**, *43*, 48−57.
(11) Tan, W. H.; Donovan, M. J.; Jiang, J. H. *Chem. Rev.* **2013**, *113*, 2842−2862.
(12) Chou, S. S.; De, M.; Luo, J. Y.; Rotello, V. M.; Huang, J. X.; Dravid, V. P. *J. Am. Chem. Soc.* **2012**, *134*, 16725−16733.
(13) Cooper, J. S.; Raguse, B.; Chow, E.; Hubble, L.; Muller, K. H.; Wieczorek, L. *Anal. Chem.* **2010**, *82*, 3788−3795.
(14) De, M.; Rana, S.; Akpinar, H.; Miranda, O. R.; Arvizo, R. R.; Bunz, U. H. F.; Rotello, V. M. *Nat. Chem.* **2009**, *1*, 461−465.
(15) Hou, Y. X.; Genua, M.; Batista, D. T.; Calemczuk, R.; Buhot, A.; Fornarelli, P.; Koubachi, J.; Bonnaffe, D.; Saesen, E.; Laguri, C.; Lortat-Jacob, H.; Livache, T. *Angew. Chem., Int. Ed.* **2012**, *51*, 10394−10398.
(16) Kong, H.; Lu, Y. X.; Wang, H.; Wen, F.; Zhang, S. C.; Zhang, X. R. *Anal. Chem.* **2012**, *84*, 4258−4261.
(17) Margulies, D.; Hamilton, A. D. *Curr. Opin. Chem. Biol.* **2010**, *14*, 705−712.
(18) Pei, H.; Li, J.; Lv, M.; Wang, J. Y.; Gao, J. M.; Lu, J. X.; Li, Y. P.; Huang, Q.; Hu, J.; Fan, C. H. *J. Am. Chem. Soc.* **2012**, *134*, 13843−13849.
(19) Severin, K. *Curr. Opin. Chem. Biol.* **2010**, *14*, 737−742.
(20) Kim, C.; Agasti, S. S.; Zhu, Z. J.; Isaacs, L.; Rotello, V. M. *Nat. Chem.* **2010**, *2*, 962−966.
(21) Giljohann, D. A.; Seferos, D. S.; Daniel, W. L.; Massich, M. D.; Patel, P. C.; Mirkin, C. A. *Angew. Chem., Int. Ed.* **2010**, *49*, 3280−3294.
(22) Kang, B.; Mackey, M. A.; El-Sayed, M. A. *J. Am. Chem. Soc.* **2010**, *132*, 1517−1519.
(23) Jones, M. R.; Osberg, K. D.; Macfarlane, R. J.; Langille, M. R.; Mirkin, C. A. *Chem. Rev.* **2011**, *111*, 3736−3827.
(24) Langille, M. R.; Personick, M. L.; Zhang, J.; Mirkin, C. A. *J. Am. Chem. Soc.* **2012**, *134*, 14542−14554.
(25) Personick, M. L.; Mirkin, C. A. *J. Am. Chem. Soc.* **2013**, *135*, 18238−18247.
(26) Rosi, N. L.; Mirkin, C. A. *Chem. Rev.* **2005**, *105*, 1547−1562.
(27) Wei, H.; Wang, Z. D.; Zhang, J.; House, S.; Gao, Y. G.; Yang, L. M.; Robinson, H.; Tan, L. H.; Xing, H.; Hou, C. J.; Robertson, I. M.; Zuo, J. M.; Lu, Y. *Nat. Nanotechnol.* **2011**, *6*, 93−97.
(28) Saha, K.; Agasti, S. S.; Kim, C.; Li, X. N.; Rotello, V. M. *Chem. Rev.* **2012**, *112*, 2739−2779.
(29) Ha, T. L.; Shin, J.; Lim, C. W.; Lee, I. S. *Chem-Asian. J.* **2012**, *7*, 36−39.
(30) Pei, H.; Li, F.; Wan, Y.; Wei, M.; Liu, H. J.; Su, Y.; Chen, N.; Huang, Q.; Fan, C. H. *J. Am. Chem. Soc.* **2012**, *134*, 11876−11879.